Modeling domestic pancake cooking incorporating the rheological properties of the batter. Application to seven batter recipes

Silvia Lorente-Bailo[a], Iñigo Etayo[b], María L. Salvador[a], Ana Ferrer-Mairal[a], Miguel A. Martínez[b,c], Begoña Calvo[b,c], Jorge Grasa[b,c,*]

[a] *Plant Foods Research Group, Instituto Agroalimentario de Aragon IA2, Universidad de Zaragoza-CITA, Miguel Servet 177, 50013 Zaragoza, Spain*
[b] *Aragón Institute of Engineering Research (i3A), Universidad de Zaragoza, Spain.*
[c] *Centro de Investigación Biomédica en Red en Bioingeniería, Biomateriales y Nanomedicina (CIBER-BBN), Spain.*

Abstract

A 2D axisymmetric model for coupled transient heat and mass transfer was developed to simulate pancake cooking on a domestic induction hob. Unlike previous models, the current model considers a variable thermal contact conductance resulting from the crust formation at the bottom of the batter. It aims to take into account the heat transfer phenomena between the pan surface and the batter influenced by the physicochemical changes that the batter undergoes during the cooking process. To quantify the variation of the heat flow that this change in the structure of the batter involves, a normalized relationship between batter viscosity and the temperature was introduced in the model. The performance of seven cereal and legume flour-based batters was evaluated in an experimental setup. The proposed model is capable of adequately predicting the weight loss and the average surface temperature of the batter using parameters related with the rheological properties of the batter and its composition.

Keywords: Pan cooking, water vaporization, batter viscosity, flour properties, finite element method

*Corresponding author: Mechanical Engineering Department, C/ Maria de Luna s/n, 50018 Zaragoza, Spain. Tel.: 34 876555288. E-mail address jgrasa@unizar.es.

1. Introduction

Pan cooking for domestic heat processing of flour cereal products has not been traditionally as widely studied as oven baking in terms of heat and mass transfer (Kokolj et al., 2017; Zhang et al., 2017; Iribe-Salazar et al., 2018). Current models are unable to adequately predict the influence of batter composition on transfer phenomena. In the case of pancake cooking models, the thermal conductivity and density of the pancake are normally expressed as a function of the batter constituents (Feyissa et al., 2011; Sanz-Serrano et al., 2017) but this dependence is not enough to explain the evaporation rates during the pan cooking of different batters.

One of the fundamental challenges that numerical modelling faces is adaptability to the following factors: cooking hardware, foods with different physico-chemical properties, different formulation of recipes, and the natural variability, as a biological material, of the food properties. The parameter uncertainty is a major problem in physical-based models (Datta, 2008). They are commonly obtained from previous models in the literature or calculated by means of optimization, i.e., minimizing the differences with experimental data (Feyissa et al., 2011; Mercier et al., 2014; Sanz-Serrano et al., 2017). However, it would be more desirable for the pancake cooking models to relate the parameters involved in the heat and mass transfer with what phenomenologically occurs and with the batter pasting properties.

Pancake cooking modelling is a complex task due to the difficulty of tracking the heat transfer phenomena between the pan surface and the batter, the noticeable physicochemical transformations of the batter during the process, and the consequent modification in the thermal contact resistance. The internal structure changes from a viscous dough to a heterogeneous structure (Cernela et al., 2015; Guibert-Martin et al., 2017). The water migrates through the outer surface in the form of liquid or vapor, so the functional properties of different flours clearly affect the moisture transport. The temperature in the contact heated surface reaches

high values, so that the proteins thermoset but the starch granules do not gelatinize. In the core, pasted starch granules act like the reinforcement material in a composite where the denatured proteins are the "mortar" (Donovan, 1977).

These changes are linked to the rheological properties. The ability of batter to retain small bubbles has been related to its viscosity, which varies with the flour (Turabi et al., 2008). The structure depends on the pasting properties of the batter (Kaur and Singh, 2005; Kaushal et al., 2012) and the consistency of the gel on the batter viscoelastic properties (Hesso et al., 2015). In turn, these rheological properties depend on the batter composition, the presence or lack of gluten, and the quantity and type of starch and fiber, among other factors. However, the rheological properties of the batter are normally not considered in the cooking modeling. Two exceptions are the work of Decindio and Correra (1995) which used the linear viscoelasticity of the batter to quantify the gas bubble expansion phenomenon, and (Lostie et al., 2002), which related the batter bulk velocity resulting from the volume expansion due to the overpressure of the gas phase with the bulk viscosity of the batter.

The main objective of this work is to relate the heat transfer phenomena between the pan surface and the batter with the physicochemical changes that the batter undergoes during the cooking process. It also aims to introduce a novel approach to simulate the domestic cooking of pancakes, allowing the application of the model to different recipes. Unlike previous models developed for pancake contact baking, this approach considers the changes in heat transfer properties as a consequence of the crust formation. Besides, it takes into account that some of the key characteristics of the model, such as the contact heating interface and water evaporation rate, are influenced by the relationship between the temperature and the batter viscosity. To achieve this goal, the basic physicochemical and rheological properties of seven batters were experimentally determined and an experimental setup was developed to reproduce the cooking process of these batters. The experimental results were used to obtain

batter-dependent parameters in the model that provided key information about the cooking performance of different compositions.

2. Material and methods

2.1. Preparation of the batters

Seven different batters were made using flours of wheat, whole spelt, whole oats, whole rice, corn, chickpea and lentil, obtained from local market. The following methods (AACC, 2000) were used for the approximate composition analysis of the flours: moisture (oven drying at 103 ^{o}C, method no. 44-15A), ash (calcination at 550 ^{o}C, method no. 08-01), lipids (extracted by Soxhlet utilizing petroleum ether as solvent, method no. 30-25), protein (Kjeldahl method, Nx5.7, method no. 46-10), fiber (method no. 32-05). Carbohydrate content was determined by the difference. The results of the different analyses are shown in Table 1.

Ingredients	Moisture	Ash	Fat	Protein	Fiber	Carbohydrate
wheat flour	14.50±0.15	0.55±0.01	1.40±0.01	11.00±0.10	2.40±0.02	70.15±0.77
whole spelt flour	11.72±0.12	1.83±0.05	3.60±0.04	13.02±0.15	5.83±0.04	64.00±0.71
whole rice flour	12.61±0.09	1.39±0.03	0.52±0.01	6.50±0.07	2.63±0.03	76.35±0.79
whole oats flour	9.66±0.12	3.98±0.04	7.89±0.09	12.70±0.11	9.67±0.10	56.10±0.59
lentil flour	8.70±0.11	2.32±0.03	1.83±0.03	24.87±0.21	8.33±0.09	53.95±0.54
corn flour	11.11±0.13	2.08±0.02	2.80±0.05	9.01±0.08	6.63±0.04	68.37±0.71
chickpea flour	8.07±0.09	2.75±0.03	5.68±0.08	20.02±0.25	13.12±0.12	50.36±0.55
Egg	77.69	0.38 (salt)	9.66	11.59	0.0	0.68
Whole Milk	88.82	0.12 (salt)	3.66	3.49	0.0	4.66

Table 1: Percentage of moisture and macronutrients of the ingredients (mean ± standard deviation). For the eggs and milk, the data were obtained from the supplier.

A pancake batter formulation containing flour (26.77 % w/w), whole milk (51.63 % w/w), pasteurized hen egg (21.03 % w/w) (Calidad Pascual, Aranda de Duero, Spain), and salt (0.57 % w/w) was used in the experiments. First, the dry ingredients (flour and salt) were mixed thoroughly. In a separate bowl, the milk and egg were mixed, and then added to dry ingredients and mixed by hand for 1 min.

2.2. Rheological analysis of batters

The rheological behavior of the batters was measured using a MCR 301 rheometer (Anton Paar Physica, Austria) equipped with serrated parallel plate geometry (50 mm diameter, 1 mm gap). The batter was left to rest for 10 min after preparation. Samples were loaded between the plates, and any excess batter outside the plate edge was removed.

For the flow measurement, shear stress values were recorded for shear rates over a range of 0.1 - 300 s^{-1} for 7.5 min. The data were fitted to the Power law model:

$$\tau = K(\dot{\gamma})^n \tag{1}$$

where τ is the shear stress (Pa), $\dot{\gamma}$ is the shear rate (s^{-1}), K is the consistency index (Pa s^n) and n is the flow index.

To study the effect of the temperature on the rheological properties, rotational tests at a heating rate of 5 ^{o}C min^{-1} from 25 ^{o}C to 100 ^{o}C were carried out at a shear rate of 200 s^{-1} (selected to guarantee the existence of a linear range according to shear rate sweeps carried out previously). Vaseline oil was applied to prevent sample drying during the test. The following indexes were determined using the software provided with the instrument: viscosity at 25 ^{o}C, η_{25^oC}; pasting temperature, T_P, (temperature at which an increase in viscosity occurs); viscosity at the pasting temperature, η_{T_P}; peak viscosity, η_{max}; and, peak temperature, $T_{\eta_{max}}$, (maximum viscosity and temperature at this point).

Oscillatory shear tests at 25 ^{o}C were conducted to characterize the viscoelastic behavior of the batter. Strain sweep tests were carried out in the range of 0.01 - 100 % at constant frequency (3 Hz). The storage modulus G', the loss modulus G'' and the loss factor $tan\delta = G''/G'$, were recorded during the test.

All the measurements were performed five times for the seven different flour and batter preparations.

2.3. Cooking conditions

Pancakes were cooked in a forged aluminium 180 mm diameter and 5 mm thickness pan with a thin bottom steel layer and a non-stick coating (Easy Induction, Kuhn Rikon, Zell, Switzerland). An induction hob (BOSCH Schott Ceran 9000440134 model, BSH, Munich, Germany) was used at power level 8.5 to supply 947 ± 4 W. The batter (110 g to obtain a pancake of 3 mm thick) was added to the pan when a uniform temperature of 230 ± 2 ^{o}C was reached, measured with an infrared thermal imager (875-2 model, Testo, Lenzkirch, Germany). All the preparations were cooked for 240 s and five replicates were performed.

The pancake weight loss during the cooking process was monitored by placing the hob on a balance (DS30K0.1L, Kern & Sohn, Balinger-Frommern, Germay) with a measurement range from 0 to 30 kg and a precision of 0.1 g that records data every 1 s. During the cooking time, a thermographic image of the upper side of the pancake was taken at 30 s intervals, and the radial temperature profiles were determined using the software Testo IRsoft (Instrumentos Testo S.A., Barcelona, Spain). A schematic diagram of the pancake cooking process is shown in Fig. 1.

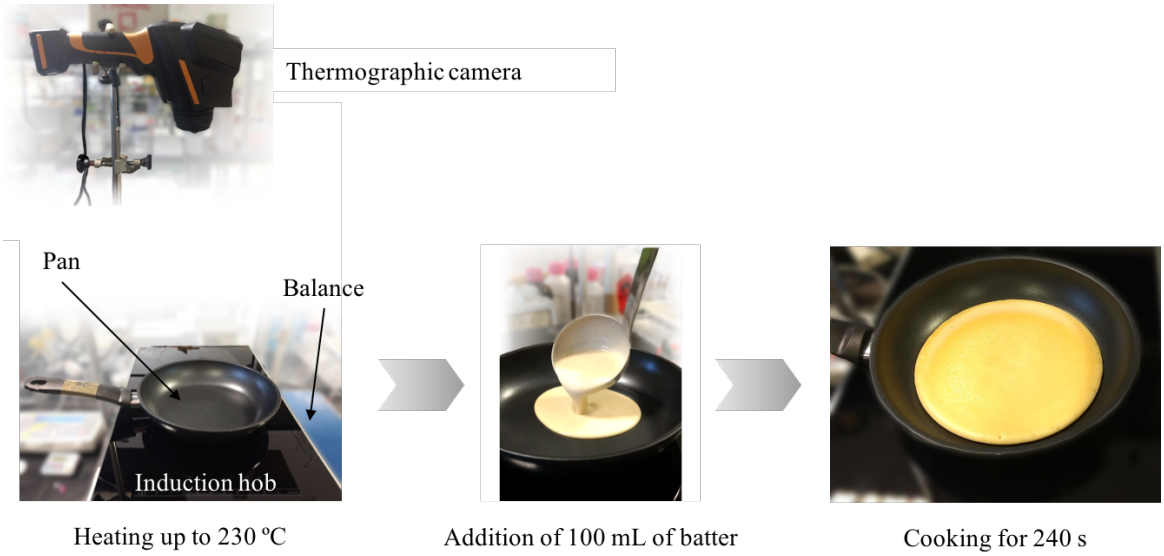

Figure 1: Experimental pancake frying setup and cooking process.

2.4. Statistical analysis

Data are presented as the mean ± standard deviation. The Statistical Package for Social Sciences (SPSS Inc, software version 22.0, Chicago, IL, USA) was used for the statistical analysis. Differences were considered significant at $P < 0.05$. Analysis of variance was performed using one-way analysis of variance (ANOVA) followed by Duncan's post hoc test for comparison of means and least significant differences (LSD).

2.5. Mathematical model

2.5.1. Hypothesis

The cooking process of pancakes was modeled as a coupled transient heat and mass transfer problem where the product was heated by contact with the hot surface of the pan. The experimental setup was recreated using the same pan geometry and the power input distribution generated by the induction hob to heat the system. Nevertheless, our approach included

several simplifying assumptions starting with an axysimmetric representation of the geometry and the heating flux power. Only energy and mass transport mechanisms were considered, assuming the pancake batter to be reasonably viscous. Moreover, the thickness was very low and no gas phase overpressure was assumed, which avoided having to account for any change of momentum of the batter bulk. The pan was heated by an inward heating flux, and heat was transferred to the batter with a very high thermal contact conductance. This drastically decreased when the viscosity increased as a crust was formed on the bottom of the batter in contact with the pan. The heat was transferred within the pancake batter by conduction, and convection to the air constituted the heat loss mechanism in the external surface. Liquid water diffused within the pancake batter, and local evaporation simultaneously occurred. Water and water vapor transport through the product were considered separately as multiphase transport species. Finally, water vapor generated in the pancake batter migrated to the top surface and subsequently diffused to the environment.

2.5.2. Heat transfer

The governing equation for the temperature evolution of the induction-heated pan was:

$$P + \lambda_{Al} \nabla^2 T = \rho_{Al} C_{Al} \frac{\partial T}{\partial t} \tag{2}$$

where P is the volumetric power density generated by the inductor at the bottom of the pan, λ_{Al} is the thermal conductivity of the aluminium, ρ_{Al} is the density and C_{Al} was the specific heat of the pan material.

Inside the pancake, considering the water energy absorption during evaporation:

$$\lambda_p \nabla^2 T = \rho_p C_p \frac{\partial T}{\partial t} + Q_{evp} \tag{3}$$

where Q_{evp} (W/m^3) is the heat dissipated by water evaporation, λ_p is the thermal conductivity,

ρ_p the density and C_p the specific heat of the pancake. To obtain the thermal conductivity of the pancake, a formula adopted from the dielectric theory developed by Maxwell (Lostie et al., 2002; Rao et al., 2005) was considered:

$$\lambda_p = \left(a\frac{X_l}{1+X_l}+b\right)\frac{(1-\varepsilon)\left(2\left(a\frac{X_l}{1+X_l}+b\right)+\lambda_{air}\right)+3\varepsilon\lambda_{air}}{(1-\varepsilon)\left(2\left(a\frac{X_l}{1+X_l}+b\right)+\lambda_{air}\right)+3\varepsilon\left(a\frac{X_l}{1+X_l}+b\right)} \tag{4}$$

This equation represents the evolution of the pancake conductivity as a function of batter porosity ε, water content per unit of dry mass X_l, air heat conductivity λ_{air} and the parameters a and b .

The pancake density was calculated as function of the density of the batter constituents and the solid, liquid and vapor mass fractions x_s, x_l and x_v (Nesvadba, 2014):

$$\rho_p = \left(\frac{x_s}{\rho_s}+\frac{x_l}{\rho_l}+\frac{x_v}{\rho_v}\right)^{-1} \tag{5}$$

Similarly, specific heat of the pancake was defined using the mass fractions as:

$$C_p = x_s C_{p_s} + x_l C_{p_l} + x_v C_{p_v} \tag{6}$$

To obtain the energy absorbed by the water during the evaporation process, the following expression was proposed:

$$Q_{evp} = \rho_p \sigma_{evp} f_v L_{evp} \tag{7}$$

where $\sigma_{evp}$was an evaporation rate constant, L_{evp} water latent heat of vaporization obtained using the least-squares fit of Torquato and Stell (1982):

$$L_{evp} = 2059.1\cdot T^{\beta} + 6604.5\cdot T^{\beta+\Delta} + 7694.3\cdot T^{1-\alpha+\beta} - 11318\cdot T - 4284.4\cdot T^2 + 2598.6\cdot T^3 \tag{8}$$

in kJ/kg, with $\alpha = \frac{1}{8}$, $\beta = \frac{1}{3}$ and $\Delta = 0.5$.

f_v was an empirical normalized function:

$$f_v = \begin{cases} exp\left(-\left(\frac{T - T_{\eta max}}{\xi}\right)^2\right), & T \leq T_{\eta_{max}} \\ 1, & T > T_{\eta_{max}} \end{cases} \tag{9}$$

Parameters $T_{\eta_{max}}$ and ξ were obtained from fitting the normalized relationship between the normalized batter viscosity and the temperature (Fig. 2). The values of these parameters for the seven batters are shown in Table 2.

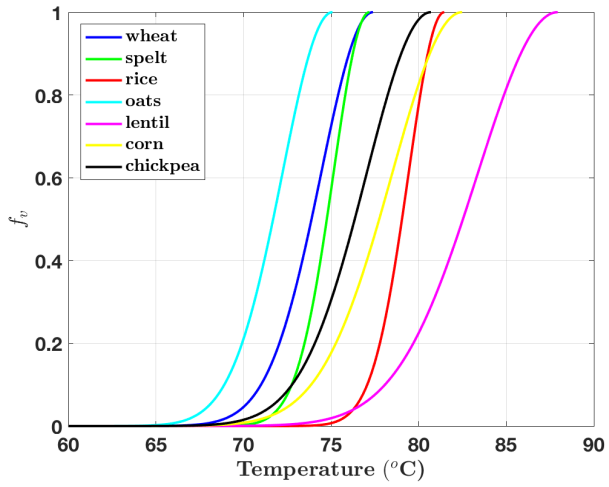

Figure 2: f_v in Eq. (9) for the batters elaborated with the different flours.

2.5.3. Mass transfer

Inside the pancake domain, the equations that govern the multiphase diffusion and water evaporation were expressed as:

$$\frac{\partial x_l}{\partial t} = \nabla(D_l \nabla x_l) - \sigma_{evp} f_v, \qquad \frac{\partial x_v}{\partial t} = \nabla(D_v \nabla x_v) + \sigma_{evp} f_v \tag{10}$$

Flours	$T_{\eta max}$ (^{o}C) fitted	ξ (^{o}C)	R^2
Wheat	74.7	3.33	0.9941
Whole spelt	75.4	2.09	0.9951
Whole rice	79.7	1.97	0.9947
Whole oats	72.4	2.78	0.9938
Lentil	80.5	2.99	0.9922
Corn	78.5	4.13	0.9859
Chickpea	76.9	2.86	0.9644

Table 2: Parameters of different batters in Eq. 9.

The constraint is $x_s + x_l + x_v = 1$. D_l and D_v are the water and vapor diffusion coefficients and $\sigma_{evp} f_v$ is the rate of water evaporation.

2.5.4. Initial and Boundary Conditions

An initial uniform temperature of 230 ^{o}C was considered for the pan; for the batter, the uniform room temperature was applied ($T_0 = 20$ ^{o}C). An input heat source was applied to the bottom region of the pan to simulate the inductive power. No vapor content was considered in this initial state.

Regarding heat transfer, the conduction mechanism was considered between the contacting surfaces of the glass and the pan through a contact conductance:

$$-\lambda_{Al} \nabla T = -\lambda_g \nabla T = h_c \left(T_g - T_{Al}\right) \tag{11}$$

where $h_c = 50$ (W/(K m^2)) is the contact conductance (Sanz-Serrano et al., 2017) and T_g and T_{Al} are the temperatures at the glass and the aluminium pan, respectively.

During cooking, the cereal or legume batter transforms from a viscous dough to a hetero-

geneous structure, which drastically modifies the thermal contact behavior with the pan. In this work, a time dependent contact conductance was introduced considering the normalized relationship between the batter viscosity and the temperature:

$$-\lambda_{Al}\nabla T = -\lambda_p \nabla T = h_{cp}(1 - f_v)(T - T_{Al}) \tag{12}$$

The bottom surface of the glass of the induction system was considered adiabatic, since the temperature of the coil and air in the real system was close to the glass temperature therefore, heat fluxes were negligible.

The natural heat convection mechanism was considered in the external wall of the pan, whereas the heat flux between the batter and the air was considered using a coefficient h_p:

$$-\lambda_p \nabla T = h_p(T - T_{air}) \tag{13}$$

Only mass flow of vapor was allowed through the top surface of the pancake:

$$-D_v \nabla x_v = k_v \rho_p (x_v - x_{v_a}) \tag{14}$$

where k_v is the vapor mass transfer coefficient; $x_{v_a} = x'_{v_a}\frac{\rho_a}{\rho_p}$ is the humidity of the surrounding air, which is expressed in terms of product mass; x'_{v_a} is the vapor fraction and ρ_a is the air density at ambient temperature (Sanz-Serrano et al., 2017).

2.6. Finite element model

An axisymmetric computational model was developed in COMSOL Multi-physics® v.5.2a to reproduce the contact baking process considering three different parts. As shown in Fig. 3, the vitroceramic glass had a thickness of 4 mm; and the aluminium pan had an internal diameter of 180 mm, 5 mm thickness and the lateral wall was 50 mm height. Finally, the pancake diameter was identical to the interior diameter of the pan and the pancake was 3 mm

thick. A mesh sensitivity analysis was conducted to find a suitable mesh size with the optimum computational efficiency for the optimization process. The selected discretization consisted of 1788 quadrilateral elements using quadratic approximation for both the mass and heat transfer (Fig. 3.a). Automatic time increments were taken by the implicit backward differentiation method and solution outcomes were saved every 1 s.

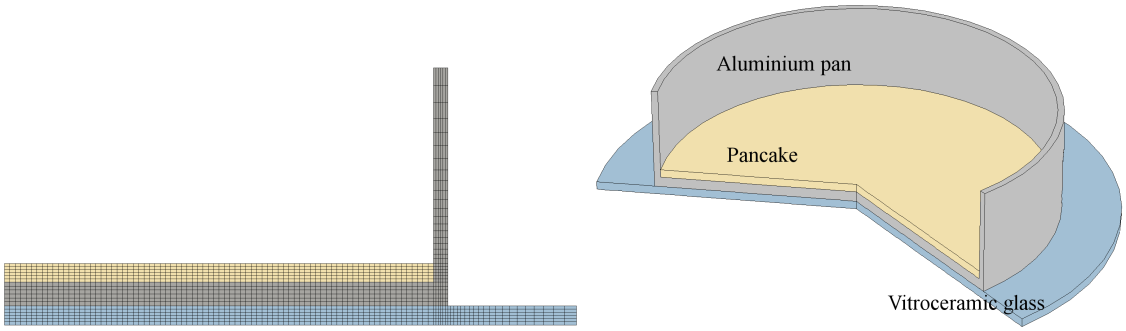

(a) (b)

Figure 3: a) Two-dimensional axisymmetric finite element mesh. b) Three-dimensional representation of the different parts of the computational model.

The power-density field acting in the pan via the induction hob was obtained from the literature (Sanz-Serrano et al., 2017) with a certain degree of modification to apply the experimental power level. The simulation time was fixed at 240 s as the experimental cooking time.

3. Results and Discussion

3.1. Experimental results

To determine the role of the composition (Table 1) in the rheological properties and the cooking behavior of the batter, several flours from different sources were selected. The flow curves, which show the variation of the shear stress with the shear rate, are shown in Fig. 4.a.

The experimental data were fitted to the power law Eq. (1), with coefficients of determination (R^2) higher than 0.997, except for the batter made with oats flour ($R^2 = 0.975$). The power law model parameters are showed in Table 3. The flow index n was 0.325 – 0.764 which denotes the deviation from being Newtonian fluids. The batters showed a typical shear-thinning (pseudoplastic) behavior, where the apparent viscosity decreased with the increase in the shear rate due to the alignment of the microstructure with the flow direction. All the samples showed low consistency K than those reported for sponge cakes (Huang and Yang, 2019). Batter consistency is related to the air incorporation and retention during baking (Turabi et al., 2008). The flow index n was significantly lower and K much higher ($P < 0.05$) in the whole spelt and chickpea batters than in the others, indicating greater pseudoplasticity and consistency in those batters under large deformations. The high amounts of protein and fiber in these flours (Table 1) reduced the amount of free water available, limiting the movement of particles in the batter, and thus giving a high consistency index. The rice batter showed the lowest consistency, which demonstrated a limited bubble holding capacity, due to the low protein content and the low solubility and functionality of these rice proteins.

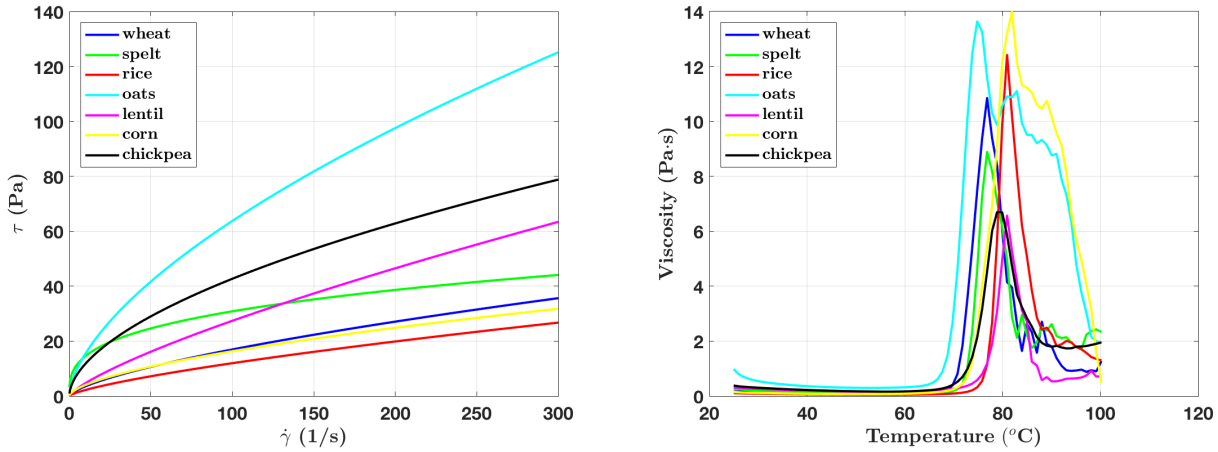

(a) (b)

Figure 4: a) Experimental results of the shear stress curves of the seven batters. b) Temperature dependence of the viscosity experimentally obtained for the seven batters.

Batter	K (Pa·s^n)	n	R^2
wheat	0.754 ± 0.014^a	0.676 ± 0.003^d	0.999
whole spelt	6.905 ± 0.089^c	0.325 ± 0.002^a	0.997
whole rice	0.411 ± 0.003^a	0.732 ± 0.002^e	1.000
whole oats	3.771 ± 0.304^b	0.614 ± 0.015^c	0.975
lentil	0.812 ± 0.010^a	0.764 ± 0.002^e	0.999
corn	1.002 ± 0.015^a	0.606 ± 0.003^c	0.999
chickpea	3.268 ± 0.040^b	0.558 ± 0.002^b	0.999

Table 3: Power law model constants for different batters: consistency index (K), flow index (n) and coefficient of determination (R^2). The values are means ± standard deviation of the replicates. The values followed by different letters in the same column are significantly different according to the Duncan's test ($P < 0.05$).

Table 4 shows the initial viscosity η_{25^oC} and the pasting properties of the different batters obtained from the temperature sweep test. The batters had a low initial viscosity, $\eta_{25^oC} < 1$ Pa·s, which was even lower than those reported for crêpes (Guibert-Martin et al., 2017). Batter viscosity should be enough to retain bubbles and prevent settling but not so high as to allow the production of pancakes as sticky textured products. Besides, the generation of convection currents in the batter during baking is dependent on the initial batter viscosity and on the evolution of bulk viscosity during heating (Martinez-Cervera et al., 2012). Rice and corn flour had the lowest viscosity values, linked to their low protein content. These results are consistent with those reported in the bibliography (Turabi et al., 2008; Guadarrama-Lezama et al., 2016; Sahagún et al., 2018). This characteristic has been correlated with a denser structure of the baked products (Baixauli et al., 2008). The legume batters showed higher viscosities than the wheat batters, as other authors have also observed (Alvarez et al., 2017), due to their richness in fiber, which are 3.5 and 5.5 times greater, respectively, for lentil and chickpea than for wheat flour (Table 1). The legume flours also have the highest protein contents, indicating a marked potential to absorb moisture and a remarkable emulsifying capacity. The oats batter showed the highest values, due to their high content of β-glucans. A high positive correlation was found between viscosity and soluble β-glucan contents (Ahmad et al., 2009; Gularte et al., 2012; de La Hera et al., 2013).

During baking at temperatures below 60 ^{o}C, the viscosity slightly decreased to a minimum value (Fig. 4.b) allowing the air bubbles to move and increase their size. When the temperature reached 60 ^{o}C, a rapid increase in viscosity was observed as previously described (Guibert-Martin et al., 2017). This increase was linked to starch gelatinization, egg protein denaturation and coagulation, and water evaporation.

The pasting temperatures ranged between 59.9 ^{o}C (wheat) and 69.2 ^{o}C (corn), and the maximum viscosity values were obtained at temperatures between 75.3 ^{o}C (oats) and 81.9 ^{o}C

Batter	η_{25^oC} (Pa·s)	η_{T_P} (Pa·s)	T_P (^{o}C)	$\eta_{\max}$ (Pa·s)	$T_{\eta_{\max}}$ (^{o}C)
wheat	0.162 ± 0.021^a	0.074 ± 0.006^a	59.9 ± 0.1^a	10.857 ± 0.915^c	77.0 ± 0.0^b
whole spelt	0.259 ± 0.017^b	0.105 ± 0.004^b	62.6 ± 0.8^b	8.896 ± 0.644^b	77.3 ± 0.6^b
whole rice	0.108 ± 0.003^a	0.072 ± 0.014^a	67.1 ± 1.9^d	12.423 ± 0.415^d	81.0 ± 0.0^d
whole oats	0.984 ± 0.122^d	0.365 ± 0.011^e	63.3 ± 0.6^{bc}	13.645 ± 1.202^e	75.3 ± 0.5^a
lentil	0.315 ± 0.027^{bc}	0.192 ± 0.008^c	64.5 ± 1.0^c	6.577 ± 1.076^a	81.3 ± 0.5^d
corn	0.153 ± 0.003^a	0.213 ± 0.002^d	69.2 ± 0.5^e	14.000 ± 0.071^e	81.9 ± 0.0^e
chickpea	0.385 ± 0.020^c	0.196 ± 0.013^c	63.4 ± 0.4^{bc}	6.698 ± 0.322^a	79.5 ± 0.5^c

Table 4: Pasting properties for different batters. The values are means ± standard deviation of the replicates. The values followed by different letters in the same column are significantly different according to the Duncan's test ($P < 0.05$).

(corn). The gluten free cereal flours, corn and rice, showed the highest pasting temperatures. Pasting properties are mainly affected by starch type and quantity, and the results indicate that starch-protein interactions decreased the T_p and η_{max} values.

The mechanical spectra for all the batters showed values of the storage modulus (G') higher than those of loss modulus (G''), typical behavior of soft gels and a weak structural network (Table 5). For wheat samples, $\tan\delta$ was 0.98, with similar moduli G' and G'', indicating more viscous and less elastic behavior. However, the value of $\tan\delta$ for the batter formulated with spelt flour was 0.27, reflecting a more structured and solid like behavior. Spelt has recently been described as having higher protein and gluten content than common wheat (Geisslitz et al., 2019). The use of legume flours (chickpea and lentil) induced a hardening effect on the batter structure (increase in G' and G'') compared to wheat batter, due to their higher content in proteins and fiber, showing a similar effect to that reported by Matos et al. (2014) for other legumes. The G' strongly depended on the strain; consequently, the loss angle increased with

the strain. The strain at which the change from solid-like ($\tan\delta < 1$) to liquid-like behavior ($\tan\delta > 1$) occurred is shown in Table 5. The strain values at $\tan\delta = 1$ was extremely high for whole spelt (12.95) and low for wheat (0.27), rice and corn (0.89). Low values have been related with an increased tendency to flow and thus with fragile batter microstructures (Guadarrama-Lezama et al., 2016).

Batter	G' (Pa)	G'' (Pa)	$\tan\delta$	Strain (%) at $\tan\delta = 1$
	in the linear range (0.1 % of strain)			
wheat	8.86 ± 0.80^{a}	8.66 ± 0.06^{ab}	0.98 ± 0.09^{e}	0.27 ± 0.02^{a}
whole spelt	279.13 ± 35.47^{c}	75.75 ± 8.25^{e}	0.27 ± 0.01^{a}	12.95 ± 0.43^{e}
whole rice	5.50 ± 0.20^{a}	4.73 ± 0.02^{a}	0.86 ± 0.03^{d}	0.89 ± 0.07^{b}
whole oats	53.44 ± 6.34^{b}	25.38 ± 1.18^{d}	0.48 ± 0.03^{b}	3.29 ± 0.25^{d}
lentil	21.56 ± 4.21^{a}	12.99 ± 2.40^{bc}	0.60 ± 0.01^{b}	1.75 ± 0.11^{c}
corn	5.62 ± 1.92^{a}	3.51 ± 0.53^{a}	0.66 ± 0.10^{b}	0.89 ± 0.07^{b}
chickpea	29.23 ± 4.38^{ab}	17.89 ± 4.02^{c}	0.61 ± 0.04^{b}	1.91 ± 0.14^{c}

Table 5: Viscoelastic measurements for different batters. The values are means ± standard deviation of the replicates. The values followed by different letters in the same column are significantly different according to the Duncan's test ($P < 0.05$).

The experimental results obtained for the average surface temperature and weight loss along the cooking of the pancake are represented in Fig. 5. The weight loss at the end of the process presented great differences depending on the type of flour (9.71% for the whole oat flour and 21.33% for the whole rice flour), whereas the temperature was very similar for all the products throughout the cooking process.

Flours	ρ_{p_0} Density (kg/m^3)	x_{l_0}	x_{s_0}	$C_{P_{p_0}}$ Specific heat (J/kg K)
Wheat	1135.11	0.6812	0.3188	3357.82
Whole spelt	1141.09	0.6738	0.3262	3344.96
Whole rice	1138.53	0.6762	0.3238	3337.73
Whole oats	1151.55	0.6683	0.3317	3335.85
Lentil	1135.66	0.6657	0.3343	3337.90
Corn	1142.06	0.6722	0.3278	3335.43
Chickpea	1143.64	0.6640	0.3360	3335.47

Table 6: Initial density, mass fractions and specific heat at ambient temperature for different batters made with the seven flour types.

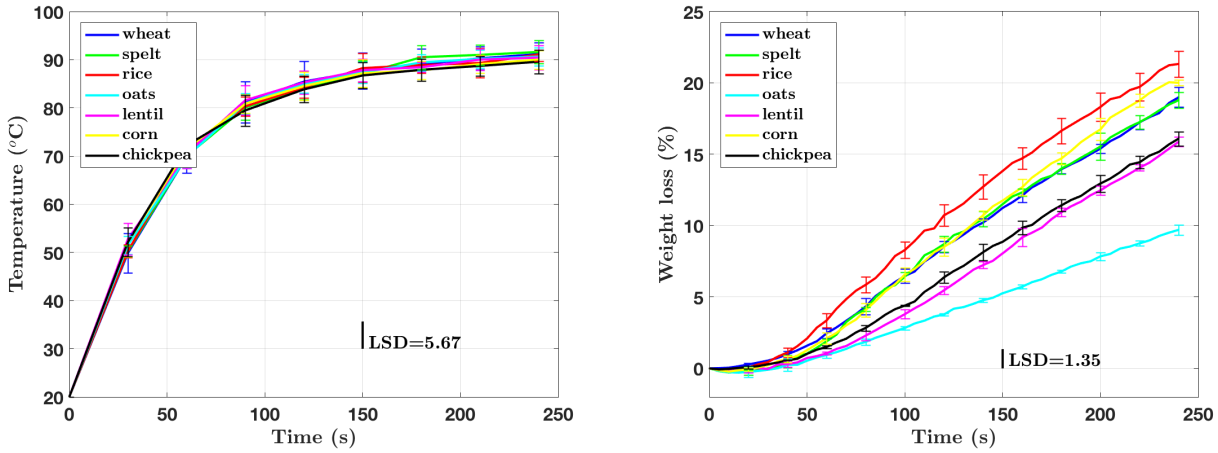

(a) (b)

Figure 5: Experimental results of the average surface temperature and weight loss. The data shown are the means (±) standard deviation of five replicates. Vertical bar = pooled least significant differences (LSD) at the 5% level.

3.2. Numerical results

Seven different models were developed using the initial batter compositions and properties as shown in Table 6. Using a gradient-based optimization algorithm implemented in the Comsol software (SNOPT), two objective functions were established based on the experimental temperature and weight loss observations. The algorithm considered eight control variables: the evaporation rate (σ_{evp}), water and vapor diffusion coefficients (D_v and D_l), the vapor mass transfer coefficient (k_v), the thermal conductivity of the pancake related parameters (a and b), the convective heat transfer coefficient between the pancake and the air (h_p) and the initial heat contact conductance (h_{cp}). These variables were selected due to their variability according to the data available in the literature.

As observed in Table 7, the highest values of σ_{evp}, D_v and D_l were obtained for the rice flour batter. These parameters governed the rate of water evaporation in Eq. (7) and the diffusion of water in the form of vapor an liquid (see Eq. (10)). As mentioned, the rice batter, due to its low protein and fiber content, showed the lowest consistency K which represented the lowest bubble holding capacity that enabled the rapid evaporation and vapor loss through the batter surface. The opposite effect was observed in the batter whole oats, rich in β-glucans. Higher consistency values were associated with the lower values of σ_{evp} and the vapor diffusivity D_v predicted by the model. Moreover, the vapor mass transfer coefficient k_v in Eq. (14) for the whole oat batter is the lowest to fit the objective of weight loss in Fig. 5.b. Due to the novelty of this study regarding the non wheat-batter flours, no previous results were found in the literature to contrast the value of these parameters. However, some previous studies proposed equivalent developments for contact baking of pancakes with wheat flour. In the work of Sanz-Serrano et al. (2017), the rate $\sigma_{evp} = 5.44 \cdot 10^{-4}$ s^{-1} was determined after an optimization process and Feyissa et al. (2011) fitted the same rate to experimental results with a mean value of $\sigma_{evp} = 11.4 \cdot 10^{-5}$ s^{-1}. The diffusivity parameters and the mass transfer coefficient

showed slight differences with those used by the above-mentioned authors. Different model assumptions, including product thicknesses and the the method to obtain other parameters, may be the cause of this discrepancy. In addition, it should be noted that the parameters provided by those previous works (Feyissa et al., 2011; Sanz-Serrano et al., 2017) are unable to reproduce the behavior of other batter compositions.

Flours	σ_{evp} (s^{-1})	D_v ($m^2\ s^{-1}$)	D_l ($m^2\ s^{-1}$)	k_v (m/s)	a (W/(m K))	b (W/(m K))	h_p (W/(m^2 K))
Wheat	$5.1623 \cdot 10^{-4}$	$9.6599 \cdot 10^{-8}$	$4.3337 \cdot 10^{-10}$	0.0421	0.8026	0.8374	14.4698
Whole spelt	$5.2813 \cdot 10^{-4}$	$1.6153 \cdot 10^{-7}$	$1.8579 \cdot 10^{-9}$	0.0555	0.8218	0.6395	14.8464
Whole rice	$6.5610 \cdot 10^{-4}$	$4.1314 \cdot 10^{-7}$	$4.4596 \cdot 10^{-9}$	0.0639	0.7776	0.5290	14.9739
Whole oats	$3.0727 \cdot 10^{-4}$	$4.2502 \cdot 10^{-8}$	$1.5381 \cdot 10^{-9}$	0.0023	0.9280	0.6370	15.2623
Lentil	$4.4458 \cdot 10^{-4}$	$9.8016 \cdot 10^{-8}$	$6.9666 \cdot 10^{-10}$	0.0459	0.8873	0.5821	14.9858
Corn	$5.7626 \cdot 10^{-4}$	$1.2582 \cdot 10^{-8}$	$1.6668 \cdot 10^{-9}$	0.0493	0.9291	0.7475	14.9846
Chickpea	$4.6349 \cdot 10^{-4}$	$8.0770 \cdot 10^{-7}$	$7.9541 \cdot 10^{-10}$	0.0474	0.8989	0.6864	14.9901

Table 7: Optimization results of the parameters in the model for the batters made with different flours.

Although not included in Table 7, the heat contact conductance h_{cp} (see Eq. (12)) was also considered in the optimization algorithm. For all the seven models analyzed, a value of $h_{cp} = 2000$ (W/(m^2 K)) was obtained. This value represented a great initial heat flux transfer between the pan and the batters, but when the temperature of the batter reached T_P this flux decreased according to the penalization function $(1 - f_v)$ in Eq. (12). Thus, the model accounted for the crust formation in the lower part of the pancake in contact with the heating surface. Physically, this region consists of a solid porous phase through which the liquid water and the vapor generated near the bottom surface move to an upper zone of uncooked batter where vapor is diffused to the environment. The crust formation modifies the thermal contact

conductance and the evolution of the heat transfer properties of the product, and consequently the rate of vapor generation in the bottom of the pancake decreases. The temperature at which these changes occur and their intensity depends on the batter characteristics, and specifically, as has been postulated in this work, on the rheological properties of the batter. On the other hand, the factors that most influence the rheological properties of the batters are the content and type of proteins and fiber. Therefore, it seems that these compositional aspects of the mass are what regulate the changes in the transport phenomena resulting from the crust formation. Although it has been experimentally described (Cernela et al., 2015; Guibert-Martin et al., 2017), to the best of our knowledge the crust formation and its consequence for the transport phenomena has not been modeled in the contact baking of flour products.

The parameters that controlled the heat conductivity of the batter in (Eq. 4), a and b did not greatly vary among the different batters. Basically, the expression that provides the equivalent thermal conductivity λ_p of the material considered the conductivity of the water together with dispersed phases (Rao et al., 2005). When the porosity of the batter increased, this conductivity decreased taking as a limit the conductivity of the air. Lostie et al. (2002) used the same expression for the thermal conductivity in the oven baking of cakes and obtained similar parameter values.

According to the values of the convection coefficient h_p, which regulated the heat exchange with the air at the upper surface of the pancake in Eq. (13), this mechanism was identical in all the models. The values predicted were in the same magnitud order as those in previous models for contact baking simulation (Feyissa et al., 2011; Sanz-Serrano et al., 2017).

The temperature evolution in the models was always whithin the standard deviation region of the experiments, which is represented by the gray area in Fig. 6 except for the initial 30 s. At the beginning of the heating process, the model stablished a non linear behavior in good agreement with that observed in previous studies (Feyissa et al., 2011; Cernela et al., 2015;

Sanz-Serrano et al., 2017). The manual operation of the infrared camera precluded sampling at high frequencies to capture the initial heating evolution. The model predicted nearly the same high temperature levels at the end of the cooking process: the chickpea flour batter had the lowest value (92 ^{o}C) and the the spelt flour batter the highest (94.8 ^{o}C). The experimental results show that the lowest value at 240 s corresponded to the chickpea flour batter with 89.6 ± 2.5 ^{o}C and the highest to the spelt flour batter with 91.6 ± 2.4 ^{o}C. In Fig. 6 the root mean square error (RMSE) between the mean of the experimental temperature evolution and the model prediction is presented for each batter. This parameter represents a measure of how close are the simulated and the experimental temperatures. For all the batters this error is equal or less than 2.7^o C.

The simulation results for the batter weight loss and the experimental replications are presented in Fig. 7. The highest amount of weight loss in the experimental results corresponded to the rice flour batter (21.3 ± 1.0 %), for which the model predicted a decrease of 23.6 %. The oat flour batter had the smallest weight loss (only 9.7 ± 0.4 %), whereas the model provided 10.8 % at the end of cooking time. All the model outcomes showed the same tendency in the weight loss evolution during the heating process, which were close to the experimental observations. As qualitatively observed, some models (i.e., lentil flour batter) perform better than others regarding the proximity of the simulated curve to the experimental one. Quantitatively, the RMSE between the mean of the experimental results and the model predictions shows the lowest value for the lentil flour batter (0.35%). A comparison with the available data in the literature shows that similar results were obtained in Sanz-Serrano et al. (2017) for the wheat flour batters but, when the thickness of the pancake increase the weight loss decreased (Feyissa et al., 2011; Cernela et al., 2015)

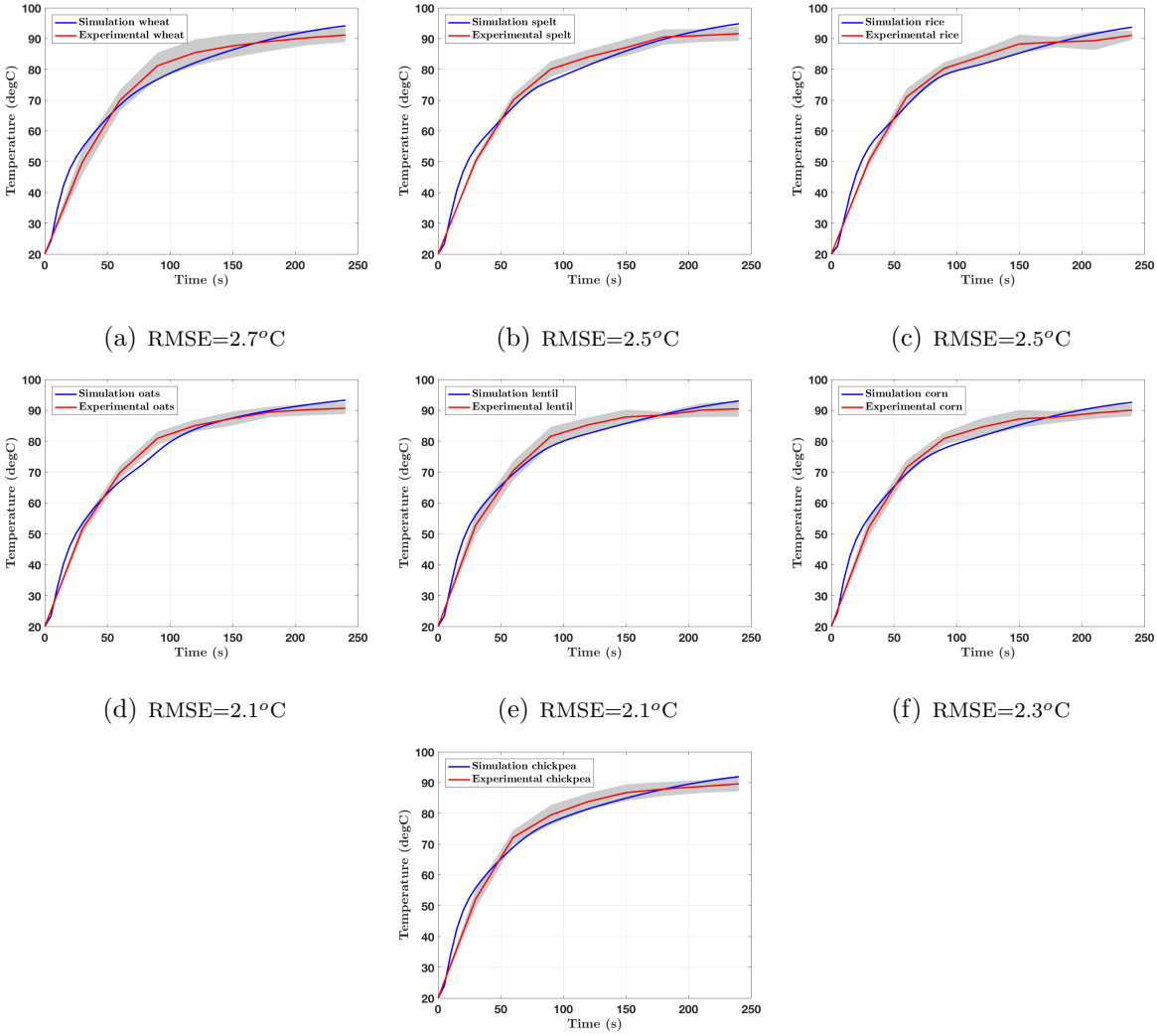

(a) RMSE=2.7^{o}C (b) RMSE=2.5^{o}C (c) RMSE=2.5^{o}C

(d) RMSE=2.1^{o}C (e) RMSE=2.1^{o}C (f) RMSE=2.3^{o}C

(g) RMSE=2.2^{o}C

Figure 6: Comparison of the simulated and measured average temperature evolutions for different batter compositions. The gray area in the figures represents the experimental standard deviation. The root mean square errors (RMSE) between the mean of the experimental results and the model prediction are presented under the figures.

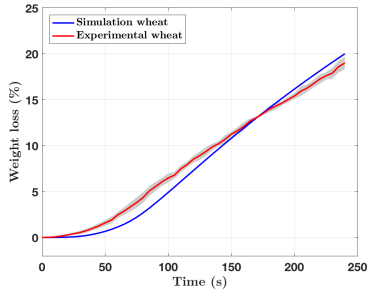

(a) RMSE=0.97%

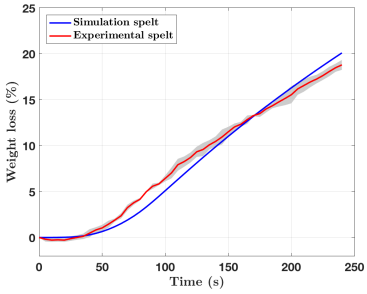

(b) RMSE=0.88%

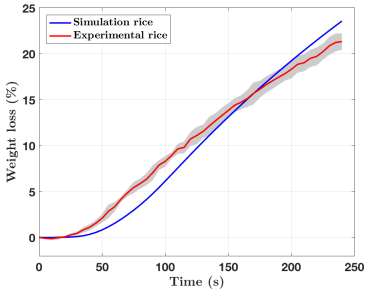

(c) RMSE=1.41%

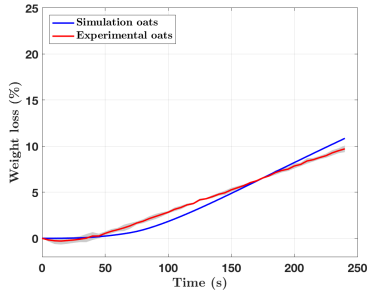

(d) RMSE=0.63%

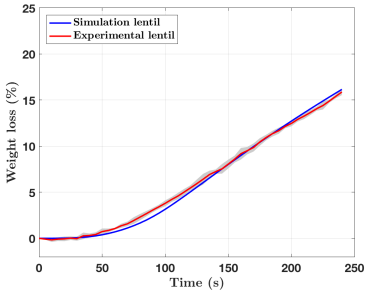

(e) RMSE=0.35%

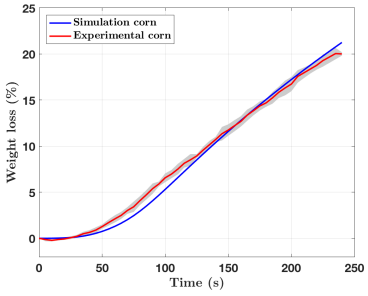

(f) RMSE=0.63%

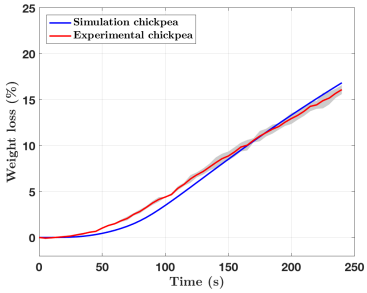

(g) RMSE=0.62%

Figure 7: Comparison between the weight loss evolution obtained with the computational simulation and the experimental results for different batter compositions. The gray area in the figures represents the experimental standard deviation. The root mean square errors (RMSE) between the mean of the experimental results and the model prediction are presented under the figures.

4. Conclusions

The laboratory setup that reproduced the domestic cooking environment enabled us to acquire repeatable temperature and weight loss measurements of the contact heating baking process of pancakes made with different flours. Seven batters made with seven different flours were analyzed. The apparent viscosity of the batter reflected a significant inverse dependence with the weight loss during the pancake cooking process. Batters containing oats and legume flours lost less weight than the wheat-based batter due to their high fiber and protein content, whereas the low protein and gluten-free batters (rice and corn) experienced a greater weight loss. No significant differences among the batters were observed for the average temperature at the upper side of the pancake.

According to the model proposed, the changes that the crust formation produces in the thermal contact conductance between the pan and the batter and in the heat transfer properties involve a decrease in the heat flux and consequently a decrease in the evaporation rate of the water at the bottom of the batter. The magnitude of these modifications and the temperature at which they occur have been related to the rheological properties of the batters, which in turn depend fundamentally on whether they are gluten-free or not and on their fiber and protein content. The values of the parameters obtained by fitting the model to the experimental data help to understand the behavior of batters of different composition and why the weight loss of these batters during the cooking process has a different evolution. These results can be useful in future studies of heat and mass transfer in cereal foods containing non-wheat flour batters.

5. Acknowledgements

This work has been funded by the Spanish Ministry of Science, Innovation and Universities through the RETOS-COLABORATION 2017 program (project RTC-2017-5965-6, ARQUE), co-financed by the European Union with ERDF; and by BSH Home Appliances Group. The

Department of Industry and Innovation (Government of Aragon) through the research group Grant T24-17R and T07-17R (co-financed by ERDF).

6. References

AACC. Methods 08-01, 30-25, 32-05, 44-15a,46-10. *AACC International. Approved Methods of Analysis 10th Ed.*, 2000.

A. Ahmad, F. M. Anjum, T. Zahoor, H. Nawaz, and A. Din. Physicochemical and functional properties of barley beta-glucan as affected by different extraction procedures. *Int. J. Food Sci. Technol.*, 44(1):181–187, enero 2009.

M. D. Alvarez, B. Herranz, R. Fuentes, F. J. Cuesta, and W. Canet. Replacement of wheat flour by chickpea flour in muffin batter: Effect on rheological properties. *J. Food Process Eng.*, 40(2), 2017.

R. Baixauli, A. Salvador, and S. M. Fiszman. Textural and colour changes during storage and sensory shelf life of muffins containing resistant starch. *Eur. Food Res. Technol.*, 226(3): 523–530, enero 2008.

J. Cernela, B. Heyd, S. Keller, J. L. Bailleul, M. N. Maillard, C. Bonazzi, and B. Broyart. Experimental study of heat and mass transfer phenomena during the contact heating of solid food models. *J. Food Eng.*, 146:99–106, 2015.

A. K. Datta. Status of physics-based models in the design of food products, processes, and equipment. *Compr. Rev. Food Sci. Food Saf.*, 7(1):121–129, 2008.

E. de La Hera, B. Oliete, and M. Gomez. Batter characteristics and quality of cakes made with wheat-oats flour blends. *J. Food Qual.*, 36(2):146–153, 2013.

394 B. Decindio and S. Correra. Mathematical-modeling of leavened cereal goods. *J. Food Eng.*,
395 24(3):379–403, 1995.

396 J. W. Donovan. A study of the baking process by differential scanning calorimetry. *J. Sci. Food*
397 *Agric.*, 28(6):571–578, Jun 1977.

398 A. H. Feyissa, K. V. Gernaey, S. Ashokkumar, and J. Adler-Nissen. Modelling of coupled heat
399 and mass transfer during a contact baking process. *J. Food Eng.*, 106(3):228–235, 2011.

400 S. Geisslitz, C.F.H. Longin, K.A. Scherf, and P. Koehler. Comparative study on gluten protein
401 composition of ancient (einkorn, emmer and spelt) and modern wheat species (durum and
402 common wheat). *Foods*, 8(409), 2019.

403 A. Y. Guadarrama-Lezama, H. Carrillo-Navas, César Pérez-Alonso, E. J. Vernon-Carter, and
404 J. Alvarez-Ramírez. Thermal and rheological properties of sponge cake batters and texture
405 and microstructural characteristics of sponge cake made with native corn starch in partial or
406 total replacement of wheat flour. *LWT-Food Sci. Technol.*, 70:46–54, 2016.

407 S. Guibert-Martin, V. Jury, B. Bouchet, G. Roellens, P. Lioret, and A. Le-Bail. Impact of the
408 baking protocol on the structure of french crepes. *J. Food Eng.*, 196:183–192, 2017.

409 M. A. Gularte, E. de la Hera, M. Gómez, and C. M. Rosell. Effect of different fibers on batter
410 and gluten-free layer cake properties. *LWT-Food Sci. Technol.*, 48(2):209 – 214, 2012.

411 N. Hesso, C. Loisel, S. Chevallier, A. Marti, P. Le-Bail, A. Le-Bail, and K. Seetharaman. The
412 role of ingredients on thermal and rheological properties of cake batters and the impact on
413 microcake texture. *LWT-Food Sci. Technol.*, 63(2):1171–1178, octubre 2015.

414 M. Huang and H. Yang. Eucheuma powder as a partial flour replacement and its effect on the
415 properties of sponge cake. *LWT-Food Sci. Technol.*, 110:262–268, agosto 2019.

R. Iribe-Salazar, R. Gutierrez-Dorado, E. Rios-Iribe, M. Carrazco-Escalante, Y. Vazquez-Lopez, O. Hernandez-Calderon, and J. Caro-Corrales. Modeling of effective moisture diffusivity in corn tortilla baking. *J. Food Sci.*, 83(8):2167–2175, 2018.

M. Kaur and N. Singh. Studies on functional, thermal and pasting properties of flours from different chickpea (cicer arietinum l.) cultivars. *Food Chem.*, 91(3):403 – 411, 2005.

P. Kaushal, V. Kumar, and H. K. Sharma. Comparative study of physicochemical, functional, antinutritional and pasting properties of taro (colocasia esculenta), rice (oryza sativa) flour, pigeonpea (cajanus cajan) flour and their blends. *LWT-Food Sci. Technol.*, 48(1):59–68, 2012.

U. Kokolj, L. Skerget, and J. Ravnik. A numerical model of the shortbread baking process in a forced convection oven. *Appl. Therm. Eng.*, 111:1304–1311, 2017.

M. Lostie, R. Peczalski, J. Andrieu, and M. Laurent. Study of sponge cake batter baking process. ii. modeling and parameter estimation. *J. Food Eng.*, 55(4):349–357, diciembre 2002.

S. Martinez-Cervera, T. Sanz, A. Salvador, and S. M. Fiszman. Rheological, textural and sensorial properties of low-sucrose muffins reformulated with sucralose/polydextrose. *LWT-Food Sci. Technol.*, 45(2):213–220, 2012.

M. E. Matos, T. Sanz, and C. M. Rosell. Establishing the function of proteins on the rheological and quality properties of rice based gluten free muffins. *Food Hydrocolloids*, 35:150 – 158, 2014.

S. Mercier, B. Marcos, C. Moresoli, M. Mondor, and S. Villeneuve. Modeling of internal moisture transport during durum wheat pasta drying. *J. Food Eng.*, 124:19–27, marzo 2014.

P. Nesvadba. *Engineering Properties of Foods*, volume 4, chapter Thermal properties of unfrozen foods. Taylor and Francis Group, 223–245, 4 edition, 2014.

M. A. Rao, S. S. H. Rizvi, and Ashim K Datta. *Engineering properties of foods*, volume 144 of *Food science and technology*. Taylor & Francis, Boca Raton, 3rd ed. edition, 2005.

M. Sahagún, A. Bravo-Núñez, G. Báscones, and M. Gómez. Influence of protein source on the characteristics of gluten-free layer cakes. *LWT*, 94:50 – 56, 2018.

F. Sanz-Serrano, C. Sagues, A.H. Feyissa, J. Adler-Nissen, and S. Llorente. Modeling of pancake frying with non-uniform heating source applied to domestic cookers. *J. Food Eng.*, 195:114–127, 2017.

S. Torquato and G. R. Stell. An equation for the latent-heat of vaporization. *Ind. eng. Chem. Fundam.*, 21(3):202–205, 1982.

E. Turabi, G. Sumnu, and S. Sahin. Rheological properties and quality of rice cakes formulated with different gums and an emulsifier blend. *Food Hydrocolloids*, 22(2):305–312, marzo 2008.

L. Zhang, C. Doursat, F. M. Vanin, D. Flick, and T. Lucas. Water loss and crust formation during bread baking, part i: Interpretation aided by mathematical models with highlights on the role of local porosity. *Dry. Technol.*, 35(12):1506–1517, 2017.